Carbon monoxide urban emission monitoring: A ground-based FTIR case study

Y. Té, Elsa Dieudonné, P. Jeseck, F. Hase, Juliette Hadji-Lazaro, Cathy Clerbaux, François Ravetta, Sébastien Payan, I. Pépin, D. Hurtmans, et al.

Carbon Monoxide Urban Emission Monitoring: A Ground-Based FTIR Case Study

Y. TÉ,* E. DIEUDONNÉ,+ P. JESECK,* F. HASE,# J. HADJI-LAZARO,+ C. CLERBAUX,+ F. RAVETTA,# S. PAYAN,* I. PÉPIN,* D. HURTMANS,@ J. PELON,# AND C. CAMY-PEYRET*

* *Université Pierre et Marie Curie, Université Paris06, and CNRS, UMR7092, LPMAA-IPSL, Paris, France*
+ *Université Pierre et Marie Curie Université Paris06, Paris, and Université Versailles St-Quentin, Versailles, and CNRS/INSU, LATMOS-IPSL, Paris, France*
# *Institut für Meteorologie und Klimaforschung-Atmosphärische Spurengase und Fernerkundung, KIT, Karlsruhe, Germany*
@ *Spectroscopie de l'Atmosphère, Service de Chimie Quantique et Photophysique, Université Libre de Bruxelles, Brussels, Belgium*

(Manuscript received 10 February 2011, in final form 18 January 2012)

ABSTRACT

The characterization and the precise measurements of atmospheric pollutant's concentration are essential to improve the understanding and modeling of urban air pollution processes. The QualAir platform at the Université Pierre et Marie Curie (UPMC) is an experimental research platform dedicated to urban air quality and pollution studies. As one of the major instruments, the ground-based QualAir Fourier transform spectrometer (FTS) provides information on the air composition of a megacity like Paris, France. Operating in solar infrared absorption, it enables the monitoring of several important pollutants involved in tropospheric chemistry and atmospheric transport around the Ile de France region. Results on nitrous oxide (N_2O), methane (CH_4), and carbon monoxide (CO) will be presented in this paper, as well as the CO measurements comparison with satellite and in situ measurements showing the capabilities and strengths of this ground-based FTS with the other instruments of the QualAir platform.

1. Introduction

The high priority on air quality research in megacities is given by atmospheric environment scientists as well as by public health authorities. In this respect, two laboratories from the Institut Pierre-Simon Laplace (IPSL)—Laboratoire de Physique Moléculaire pour l'Atmosphère et l'Astrophysique (LPMAA) and Laboratoire Atmosphères, Milieux, Observations Spatiales (LATMOS)—have joined their efforts to develop an innovative experimental research platform for the Quality of the Air (QualAir; see http://qualair.aero.jussieu.fr) that is dedicated to urban atmospheric research, providing precise information on the pollutant concentrations distribution (gas species and aerosols). The QualAir station, located on the University Pierre et Marie Curie (UPMC) campus in the center of Paris (48°50′47″N, 2°21′21″E, 60 m above sea level) is mainly composed of a laboratory connected to the roof terrace on which several instruments collect different atmospheric signals (solar radiation, ambient air, etc.). The following different measurement techniques are employed: passive remote sensing with the QualAir Fourier transform spectrometer (FTS; Té et al. 2008, 2010); active remote sensing with the Cloud and Aerosol Microlidar (CAML) for backscattering coefficient, clouds, and aerosols properties, etc. (see http://www.cimel.fr); and in situ measurement of the carbon monoxide concentration with the CO11M analyzer from Environnement SA (see http://www.environnement-sa.fr). In this paper, we present the results on nitrous oxide (N_2O), methane (CH_4), and carbon monoxide (CO) species. Both N_2O and CH_4 are both greenhouse gases, and the quantification of their concentration is crucial for global warming impact studies (climate models). CO is a good indicator of anthropogenic pollution because natural sources are comparatively small. The measurement of atmospheric pollutants like CO is a key to improving our understanding of urban air pollution processes. The CO observations made by the instruments listed above are intercompared as well as compared to the satellite Infrared Atmospheric Sounding Interferometer (IASI)

Corresponding author address: Yao Veng Té, LPMAA/UPMC/CNRS, Case 76, 4 Place Jussieu, 75005 Paris, France.
E-mail: yao-veng.te@upmc.fr

DOI: 10.1175/JTECH-D-11-00040.1

Meteorological Operation (MetOp) results (Tournier et al. 2002; Blumstein et al. 2004) to check the consistency of the atmospheric pollutant concentration monitoring, especially in the free troposphere (see section 4).

2. QualAir FTS description

The QualAir platform Fourier transform spectrometer is a Michelson interferometer with a maximum optical path difference of 258 cm. It is based on an Integrated Forecast System (IFS) 125HR model from Bruker Optics (see http://www.brukeroptics.com), which is adapted for ground-based atmospheric measurements (see Té et al. 2010 for more details). Connected to a sun tracker on the roof terrace, the QualAir FTS operates in the solar absorption configuration and enables the detection of a large number of atmospheric pollutants. When locked on the solar disk center using a photodiode system, the sun tracker collects the solar radiation after transmission through the atmosphere and transfers it to the lower-level experimental room before injecting it into the interferometer. At full spectral resolution (0.0024 cm^{-1}), and depending on the atmospheric conditions, each solar spectrum is recorded between 3 min (with very small local clouds) and 10 min (for clear sky). The solar spectra are sorted and those recorded in presence of clouds are excluded. The spectra contain many rovibrational signatures of the atmospheric constituents, including pollutants.

To optimize the signal-to-noise ratio and to focus on specific species of interest, appropriate optical filters and detectors combination has to be chosen: a mercury cadmium telluride (MCT) detector with a 7.1–10-μm optical filter (cf. Fig. 1, top panel) is used to monitor, for example, ozone (O_3), water (H_2O), dichlorodifluoromethane [CCl_2F_2 (CFC-12)], etc.; an indium antimonide (InSb) detector with an optical filter from 3.8 to 5.1 μm (cf. Fig. 1, middle panel) is used to monitor CO, carbonyl sulfide (OCS), carbon dioxide (CO_2), N_2O, CH_4; and an InSb detector with a 3.1–4.2-μm optical filter (cf. Fig. 1, bottom panel) is used to monitor NO_2, hydrogen chloride (HCl), ethane (C_2H_6), formaldehyde (H_2CO), etc. In this paper, we focus on the N_2O, CH_4, and CO species using the second type of detector and optical filter for solar spectra that were recorded between 1 July 2009 and 25 May 2011.

3. QualAir FTS results

a. Retrieval method

The absorption lines of the species observed in the solar spectra recorded by ground-based spectrometers can be used to retrieve their concentration in the atmosphere by processing the experimental spectra or spectral microwindows with appropriate radiative transfer and inversion algorithms (Té et al. 2010; Rinsland et al. 2006; Wunch et al. 2006; Sussmann et al. 2005; Hase et al. 2004; Barret et al. 2003; Zhao et al. 1997). In the case of direct solar absorption, the radiative transfer algorithm is based on the Beer–Lambert law,

$$I_{\tilde{\nu}}(s) = I_{\tilde{\nu}}(0)T_{\tilde{\nu}}(0,s). \quad (1)$$

Here $I_{\tilde{\nu}}(0)$ is the incident solar intensity at the top of the atmosphere; $I_{\tilde{\nu}}(s)$ is the intensity at the position s along the absorption path; and $T_{\tilde{\nu}}(0,s)$ is the atmospheric transmission between the positions 0 and s, which depends on several parameters like spectroscopic line parameters of the relevant atmospheric species [position, intensity, pressure line shift, and broadening parameters; see Rothman et al. (2009)]; pressure and temperature vertical profiles (see http://www.ecmwf.int and http://www.ncep.noaa.gov); the a priori vertical profile of each studied species (U.S. Air Force 1976; http://waccm.acd.ucar.edu); the instrument line shape; the H_2O continuum (Clough et al. 2005); and the geometry of the line of sight. The atmospheric theoretical spectrum calculated by the radiative transfer model is compared and fitted to the measured solar spectrum through the inversion algorithm using a least squares minimization method in order to provide the total column or the vertical profile. For this study, we have used the PROFILE FIT (PROFFIT) algorithm developed by Hase et al. (2004) to analyze the QualAir FTS data. PROFFIT is a code for the analysis of solar absorption spectra. It has extensively been compared to SFIT2, which is a code widely used by the FTIR community in the Network for the Detection of Atmospheric Composition Change (NDACC; see http://www.ndsc.ncep.noaa.gov) for the same purpose, and excellent agreement between the two codes has been found (Hase et al. 2004). PROFFIT has been applied by various scientists for solar absorption spectra analysis. The radiative transfer model included in PROFFIT contains a sophisticated model of the solar background spectrum (Hase et al. 2006), allows it to include a detailed characterization of the spectrometer's instrumental line shape (Hase et al. 1999; Schneider and Hase 2008), and is able to handle non-Voigtian line shape models (Schneider and Hase 2009; Duchatelet et al. 2010). The inverse code of PROFFIT supports both optimal estimation and Twomey–Tikhonov constraints and is able to perform the retrieval in log[volume mixing ratio (VMR)] space, which is required to handle trace gases with strong variability in an optimal manner, such as, for example, H_2O and CO (Schneider et al. 2006).

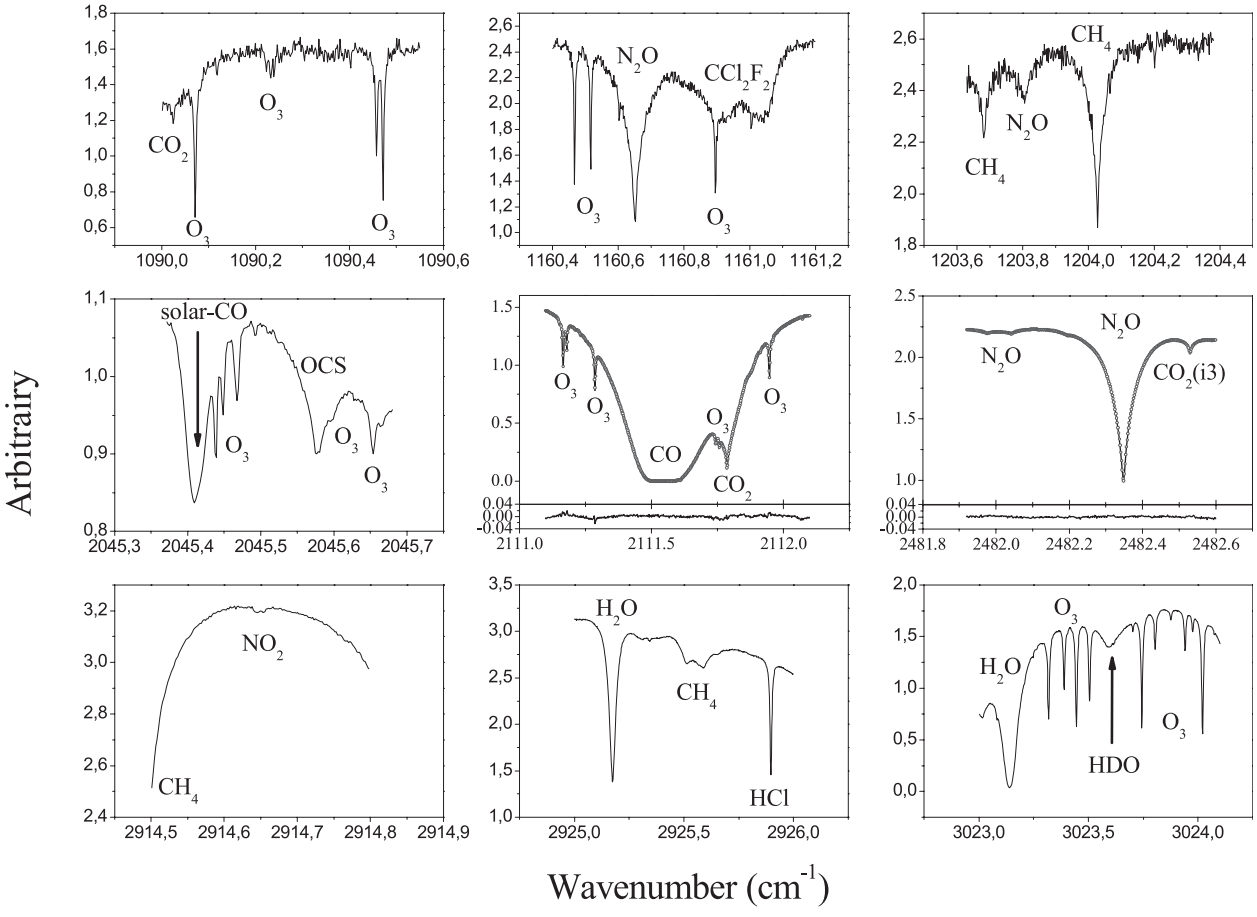

FIG. 1. Some of the species observed by the QualAir FTS. Simulated spectra (open circles) and residuals (below) are shown.

Furthermore, PROFFIT is able to apply interspecies constraints for isotopic work, for example, the retrieval of HDO/H_2O ratio profiles (Schneider et al. 2010). In the case of QualAir FTS, the atmosphere is modeled by 49 altitude levels where the a priori VMR profiles are sampled in a parts per million by volume (ppmv) unit (cf. opened stars curve for the CO a priori profile in Fig. 7). The layer's altitude grid is close enough to characterize the planetary boundary layer (PBL) properly.

Figure 2 presents the VMR averaging kernels (AK) for CO, which are calculated for each level of the altitude grid (Rodgers 1990). To make the analysis of the AK information content easier, we have only presented some of the averaging kernels' curves (gathered in two distinct groups according to their peak sensitivity), showing two regions of high sensitivity for these retrieval levels clearly. Information is considered to be independent when the full widths at half maximum of the different functions are well separated. This is the case for the two independent information points shown in Fig. 2—the first one in the PBL around 500–1000 m and the second in the troposphere around 8–9 km. We have noticed a third information point at a higher altitude in the stratosphere, which is not discussed in this paper. In the PBL, the five first AK functions are superposed. Thus, the information on the PBL is partially smoothed out (see the section 4c for improving the detection of pollutant in the PBL by atmospheric modeling and using different QualAir platform instruments synergy).

b. Retrieval errors

Two kinds of errors can affect our recorded solar spectra and the retrieval process: random errors and systematic ones (Rinsland et al. 1998, 1999, 2000). Random errors are the uncertainties in temperature profiles, the solar zenith angles (SZAs), the effect of the instrumental noise, and the error in the absorption of interfering solar lines calculation. Systematic errors include the spectroscopic parameters uncertainty, the a priori profile, and the errors in the instrument line shape (ILS) function. Some errors sources can be considered both random and systematic, for example, temperature profile, SZA, interfering solar lines, etc. Effectively, the sun tracker's quadrant sensors may not be well aligned and

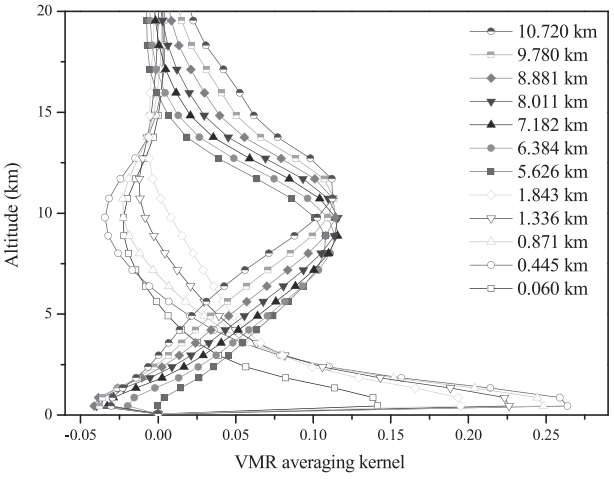

FIG. 2. Some of the VMR averaging kernels obtained for CO using both CO microwindows and for each altitude of the a priori profile.

TABLE 1. CO retrieved total column uncertainties.

Random errors	
Error source	CO error (%)
Temperature	1.8
Instrument noise	<1
Solar zenith angle	1.1
Interfering solar lines	<1
Total random error	2.4
Systematic errors	
Spectroscopic parameters	3–6.8
A priori profile	<1
Instrument line shape	<1
Total systematic error	3.1–6.9

may introduce a part of systematic errors in the line of sight (LOS) determination and some random errors resulting from the accuracy of the pointing. In Table 1, we report the retrieval errors resulting from both random and systematic errors on the retrieved CO total columns. Next, we describe the procedures and assumptions used in generating the uncertainty through the retrieval algorithm PROFFIT.

National Centers for Environmental Prediction (NCEP) temperature profiles were calculated for the date and the location of the observations. They are assumed to be nominal. New retrieval was performed by adding 2 K to the temperature at each altitude of the temperature profile (Rinsland et al. 1998). The retrieval error is represented by the magnitude of the difference between the nominal CO total column and the shifted one. For CO, the error resulting from 2-K temperature uncertainty is about 1.8%.

Each solar spectrum is generated from coadded scans. Most of the time, it is two coadded scans. The air mass is calculated from the average recording time. Errors are introduced by these approximations to estimate the air mass and by the uncertainties in the time reading and stamping of the individual files. We have considered an uncertainty of 30-s corresponding to an uncertainty of 0.004 rad in the LOS direction for spectra with an SZA higher than 70° (Rinsland et al. 1999). Calculations showed an SZA error effect less than 1%.

To evaluate the instrumental noise contribution, we have generated 10 synthetic spectra with random noise [the same magnitude as the real instrumental noise (Rinsland et al. 1998)]. New retrievals were performed using these spectra. No specific bias was observed with respect to the nominal total column. The maximal difference between random noise spectra and the nominal one provided a retrieval error of about 1.1%.

It is important to take into account all interfering atmospheric lines; the H_2O continuum; and the overlapping wing absorption of strong lines such as H_2O, CO_2, CH_4, etc. PROFFIT has integrated these considerations and allows the retrieval of several atmospheric species at the same time. However, the modeling of the solar lines (solar CO lines, e.g.) may be inaccurate and may introduce errors (Rinsland et al. 2000). We calculated a retrieval error less than 1% for a solar lines intensity uncertainty of 5% and a spectral scale uncertainty of.$\Delta\tilde{\nu}/\tilde{\nu} \sim 10^{-6}$.

For all atmospheric lines, we use spectroscopic parameters from the High Resolution Transmission (HITRAN) database. The high quality of the CO parameters in HITRAN 2008 provides a line intensity uncertainty from 2% to 5% and an air-broadening γ_{air} uncertainty from 1% to 2% (Rothman et al. 2009). Calculation provided a retrieval error from 3% to 6.8%.

The true and a priori profiles have structures finer than the measurement of vertical resolution determined by the averaging kernels. The profile information derived from the retrieval process is not sufficient to choose the a priori profile independently. We use Whole Atmosphere Community Climate Model (WACCM) profiles for the latitude and longitude centered at the QualAir platform for a priori profiles. To observe the dependence of the a priori profile on the retrieval (Rinsland et al. 2000), we retrieved the CO total columns with a modified a priori profile by adding 20% to the VMR at each altitude. The influence of the a priori profile introduced an error smaller than 1%.

To estimate the effect of uncertainty in knowledge of the instrument line shape function, we generated a synthetic spectrum by assuming a theoretical ILS. From this synthetic spectrum, the corresponding interferogram is calculated and multiplied with a linear function varying from 1 at the zero path difference (ZPD) to 0.8 at the maximum path difference (MPD; cf. Park 1983). This calculation simulates an apodization function error that increases linearly from zero at the ZPD to 20% at the MPD. The retrieval error resulting from this ILS apodization error is less than 1%.

In conclusion, we estimated a total random error of 2.4% and a total systematic error of 6.9%. The precision of the CO retrieval through PROFFIT is about 9.3%, less than 10%. It is the superior limit of the retrieval uncertainty.

c. Retrieval results

Different microwindows are used to retrieve the atmospheric species concentration (Meier et al. 2004): 2481.3–2482.6, 2526.4–2528.2, 2537.85–2538.8, and 2540.1–2540.7 cm^{-1} for N_2O; 2613.7–2615.4 cm^{-1} for CH_4; and 2110.4–2110.5 and 2111.1–2112.1 cm^{-1} for CO. The sensitivity of these windows to PBL conditions is variable. For CO, the left and right wings of a strongly saturated line (in the second microwindow) are most sensitive to the PBL. Conversely, the weak line (hence, unsaturated line) of the first microwindow is more sensitive to VMR profile information at higher altitudes. The vertical VMR profiles of N_2O, CH_4, and CO have been retrieved using the same solar spectrum. These spectra are recorded on 1 July 2009 between 0641 and 1240 UTC. For the CO comparison with satellite, other spectra between 13 July 2009 and 25 May 2011 are only used between 0900 and 1100 UTC (around the satellite overpasses). The total columns of these three species can be calculated from their respective VMRs using the temperature and pressure.

These three atmospheric constituents discussed are chosen for their differences in emission sources, lifetime, etc., and their possible correlations. Both N_2O and CH_4 have biogenic and anthropogenic sources with quite long lifetimes (around 150 and 10 years, respectively). The sources of atmospheric CO are mainly due to human activities (hydrocarbons from incomplete combustion). The oxidation of CO by the hydroxyl radical (OH) is more effective as compared to the reaction with CH_4 (Delmas et al. 2005), leading to a shorter lifetime of 2 months and a large variability of CO. Species distributions are strongly influenced by both chemical and dynamical processes. For long-lived trace gases such as CH_4 and N_2O, where the mixing occurs on time scales much shorter than their photochemical lifetimes, their distributions should be compact and collapse to a single value (Plumb et al. 1992). Vertical concentration distributions with high vertical resolution obtained from balloon and aircraft in situ measurements are used to track intrusion and horizontal transport of the air masses (Kondo et al. 1996; Michelsen et al. 1998; Fischer et al. 2000). Ground-based remote sensing instruments have limited vertical resolution. The vertical independent information contained in the recorded solar spectra is well mixed along the line of sight (see the averaging kernels analysis in section 3c). Thus, we use the total columns correlation (containing all information in the line of sight) to detect local sources. Figure 3 shows the expected good correlation of the total columns between CH_4 and N_2O, proving no intense anthropogenic sources of N_2O (nitrogen fertilizer) or CH_4 in Paris. There is no correlation between CO and the other two tracer species, as shown in Fig. 4 (open stars representing N_2O and dark circles CH_4), proving the large local anthropogenic source of CO in Paris.

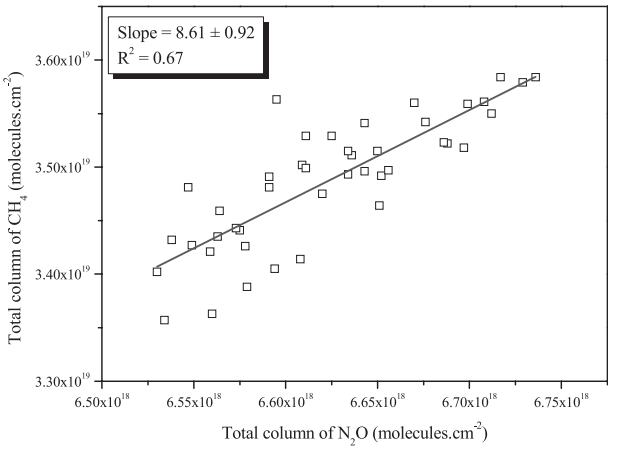

FIG. 3. Total columns correlation between N_2O and CH_4.

4. Intercomparison results

a. Satellite MetOp IASI

To demonstrate the good consistency of our QualAir FTS results, a comparison with the CO products (L2) generated from the IASI sounder on the MetOp satellite is performed. The total column data were generated from the IASI radiance spectra using the Fast Optimal Retrievals on Layers for IASI (FORLI) retrieval algorithm (Clerbaux et al. 2009; George et al. 2009) with a relative uncertainty between 4% and 10%. George et al. (2009) shows the MetOp IASI averaging kernels presenting two maxima, at the surface and around 6 km, which are very similar to our averaging kernels (cf. Fig. 2). MetOp IASI has a swath of 30 fields of regard of

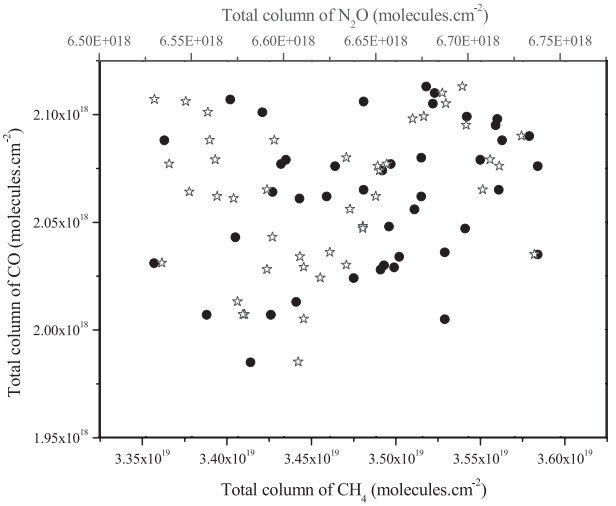

FIG. 4. Total columns correlation between CO and N_2O (open stars) and between CO and CH_4 (circles).

50 km × 50 km comprising four off-axis pixels of 12-km diameter each (Turquety et al. 2007). Only overpasses around Ile de France (±0.5° in latitude and longitude) are used. This corresponds to about a 100 km × 100 km square region centered on the QualAir platform location. Table 2 shows the average total columns obtained by QualAir FTS and MetOp IASI between July 2009 and May 2011. The QualAir FTS results are in good agreement with those from MetOp IASI within 10% discrepancy except for 5 days. For 11 October 2010, 22 April 2011, and 4 May 2011, MetOp IASI observed less CO. All overpasses for these days were more than 30 km away from the QualAir platform. MetOp IASI sounded the far-outlying suburbs and rural areas were less polluted than the urban zones. For 13 and 16 July 2009, the total columns inside Paris are larger for MetOp IASI, more than 30%, as compared to the QualAir FTS averages. Maps obtained by the chemistry-transport model (CHIMERE) model (Vautard et al. 2001; Schmidt et al. 2001; Honoré et al. 2008) show CO pollution plumes from the north and northwest of Paris, respectively, for 13 and 16 July. These pollution plumes were detected by MetOp IASI because of the large MetOp IASI footprint of 12-km diameter, whereas the QualAir FTS IFOV looked in the opposite southeast direction at about 0930 UTC. Overpasses for downtown provide a better colocation with the QualAir FTS IFOV, and thus a better agreement. The total columns inside Paris are, as expected, slightly higher, shown with respect to the larger CO emissions in urban areas.

Figure 5 presents the MetOp IASI footprints for the case study around the Ile de France with the total columns in 10^{18} molecules per square centimeter on 1 July 2009. The closest overpass is point 5 (around 10 km from the platform), but it occurred at 1957:42 UTC and there was no QualAir FTS measurement because of sunset around that time. The second closest instantaneous fields of view (IFOVs) of IASI are points 1 and 2. Both are around 15 km away from Jussieu (the Argenteuil and Orly areas, respectively). Thus, the UPMC campus is in the middle of these two points. The overpass was at 1011:28 UTC with a mean CO total column derived from orbit of $(2.11 \pm 0.09) \times 10^{18}$ molecules per square centimeter. The closest solar spectrum recorded from the ground by the QualAir FTS was at 1012:06 UTC (3 min of acquisition duration) and provided a CO total column of 2.06×10^{18} molecules per square centimeter. To check the CO total column variability, the mean CO total column obtained by the QualAir FTS for the whole day was $(2.06 \pm 0.04) \times 10^{18}$ molecules per square centimeter as compared to $(2.05 \pm 0.16) \times 10^{18}$ molecules per square centimeter, the mean value from the eight overpasses. For the QualAir FTS total columns, the uncertainty is the standard deviation of all data used to calculate the mean value. This standard deviation reveals the variation of the total columns retrieved by the PROFFIT algorithm. The stronger variability observed by MetOp IASI is probably due to the time discrepancy and the different areas sounded by the satellite instrument (e.g., point 3 versus point 8). The comparison between ground-based high-resolution

TABLE 2. Total columns obtained by QualAir FTS and MetOp IASI.

Date	QualAir FTS	IASI-a(*)	IASI-b(**)
1 Jul 2009	2.06 ± 0.04	2.05 ± 0.16	2.11 ± 0.09
13 Jul 2009	1.73 ± 0.02	2.23 ± 0.09	2.73 ± 0.11
16 Jul 2009	1.62 ± 0.03	1.90 ± 0.09	2.43 ± 0.11
16 Feb 2010	2.45 ± 0.05	2.40 ± 0.14	2.53 ± 0.14
2 Mar 2010	2.57 ± 0.05	2.68 ± 0.11	2.63 ± 0.10
7 Jul 2010	1.95 ± 0.05	2.15 ± 0.10	2.09 ± 0.10
11 Oct 2010	1.81 ± 0.03	1.62 ± 0.11	None
8 Mar 2011	2.77 ± 0.05	2.35 ± 0.12	2.44 ± 0.10
19 Apr 2011	2.21 ± 0.04	1.91 ± 0.06	2.07 ± 0.05
20 Apr 2011	2.38 ± 0.03	2.18 ± 0.07	2.22 ± 0.05
21 Apr 2011	2.23 ± 0.03	1.94 ± 0.06	2.07 ± 0.05
22 Apr 2011	2.15 ± 0.06	1.93 ± 0.06	None
26 Apr 2011	2.54 ± 0.04	2.10 ± 0.06	2.22 ± 0.05
4 May 2011	2.83 ± 0.04	2.48 ± 0.06	None
5 May 2011	2.13 ± 0.02	2.36 ± 0.06	2.38 ± 0.05
6 May 2011	2.33 ± 0.05	None	None
12 May 2011	2.16 ± 0.05	None	None
13 May 2011	2.35 ± 0.03	2.28 ± 0.05	2.26 ± 0.05
25 May 2011	2.06 ± 0.03	1.97 ± 0.05	2.04 ± 0.05

* All morning overpasses around Ile de France (±0.5° in latitude and longitude corresponding to a 100 km × 100 km square region centered on QualAir platform location).

** Overpasses inside Paris "downtown" (<±0.15° in latitude and longitude).

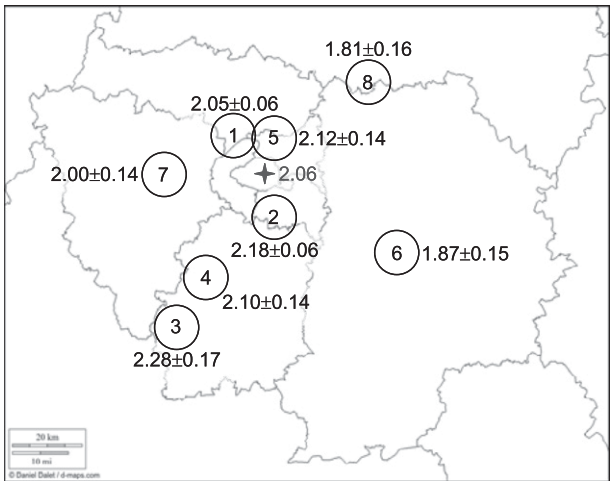

FIG. 5. Location of MetOp IASI footprints (overpasses in circles) around Ile de France region on 1 Jul 2009. The location of the QualAir platform is indicated (star). The numerical total columns are in 10^{18} molecules per square centimeter.

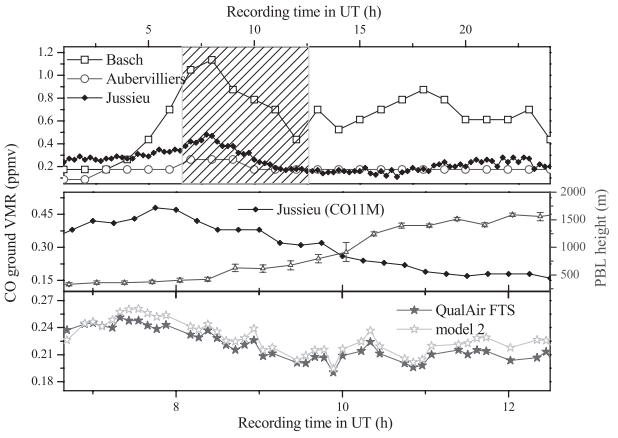

FIG. 6. CO ground VMR comparison between (bottom) remote sensing and (middle), (top) in situ measurements. (middle) Boundary layer height was obtained by the CAML (open triangles). (middle), (bottom) Data in the top panel cross-hatched time period are shown.

solar FTIR and thermal infrared nadir sounding from orbit is thus satisfying.

b. CO11M analyzer

The CO11M analyzer uses the CO infrared absorption band around 4.67 μm to provide the CO in situ concentration. The atmospheric air is taken from the terrace [by a polytetrafluoroethylene (PTFE) tube], led into the analyzer in the experimental room one floor below, and analyzed in a multipath (28 reflections) absorption cell or sampler chamber. The accuracy of the CO11M analyzer is ± 50 parts per billion by volume (ppbv) on one single measurement. Figure 6 shows (in the top panel) the CO ground VMR obtained by the association interdépartementale pour la gestion du réseau automatique de surveillance de la pollution atmosphérique, et d'alerte en région d'Ile-de-France (AirParif) network (for Basch in dark open squares and Aubervilliers in open circles) and the CO11M at the Jussieu campus (in diamonds). The middle and bottom panels represent the cross-hatched time period. The QualAir FTS results are shown in stars. The QualAir FTS ground VMR corresponds to the averaged VMR of the lower levels in the retrieved vertical profile of CO (from 0.06 to 1 km, see section 3a). On the top panel, we notice a pollution peak detected at the same time (0745 UTC) at the Basch station and by the CO11M. However, the measured VMR at both locations is different because the Basch station (see http://www.airparif.fr) is located along a high-traffic axis with more than 100 000 vehicles per day (2004 statistics). The UPMC campus is surrounded by streets but the traffic is less intense. As seen in the top panel, the CO11M at Jussieu is operating in an intermediate location between an observation site in a high-traffic zone, for example, Basch, and a site in the suburbs, for example, Aubervilliers, which should provide a good CO background measurement. Between the middle (CO11M) and bottom (QualAir FTS) panels, we observe a good time relation for the daily CO pollution peak resulting from urban traffic rush hours. The time difference is quite small, around 20 min, which can be explained by the different measurement techniques (remote sensing and in situ). The air masses probed by the two instruments are slightly different and depend on the local wind velocity and direction, but also on the line-of-sight geometry used by the remote sensing technique. Thus, the absolute in situ pollution peak value (0.48 ppmv) cannot match the value retrieved by the QualAir FTS (maximum at 0.25 ppmv) perfectly. The strong local variations near the ground are smoothed out into the atmospheric layers through the retrieval model. One of the difficulties of ground-based infrared remote sensing in solar absorption is the limited vertical resolution because the information from each atmospheric layer is merged into the overall line profile. Thus, the retrievals at different levels are not independent (Rodgers 1990; Zhao et al. 2002; Rinsland et al. 2007; cf. Fig. 2). However, after the pollution peak detected by the in situ sensor, we notice globally the same daytime decrease in both instruments. The mean values are quite similar: 0.27 ppmv for in situ measurements and 0.22 ppmv for remote sensing ones. The background values are also consistent within the accuracy of the instruments: 0.16 ppmv for the CO11M analyzer and 0.20 ppmv for the QualAir FTS. The data of the ''model 2'' in the bottom panel of the Fig. 6 are discussed in the next section.

c. Boundary layer analyses

1) MICROLIDAR CAML

The CO pollution peak value can vary depending on the atmospheric state and on the PBL's dynamics for that day, and this information can be provided by the microlidar CAML. It is a commercial instrument from CIMEL Electronique that uses an output laser at 532 nm and produces information on the vertical profile of the backscattering coefficient in the boundary layer, and on the optical and dynamic properties of clouds and aerosols. Atmospheric stratification is determined using the range-corrected signal averaged over 20 min. The top of the boundary layer is defined as the altitude where the signal gradient reaches its minimum (Menut et al. 1999). When a cloud caps the boundary layer, the cloud base is taken to be the top of the boundary layer (cf. Fig. 6, opened triangles). Cloud base is defined as the altitude of where the signal gradient is maximum. Uncertainty on the value of the boundary layer top value is defined as the altitude range where the absolute value of the signal gradient is higher than 80% of its maximum value. The minimum boundary layer top that can be observed by this instrument is 0.3 km.

2) MODEL 1 DESCRIPTION

The planetary boundary layer is the first and lowest atmospheric layer from the ground up to several hundred meters. The atmospheric dynamics in the PBL are strongly determined by erratic changes in wind direction and velocity (turbulence), which depend on the local orography; the meteorological conditions; the solar radiation; etc. As a consequence, the atmospheric constituents are well mixed in the PBL provided they have a much longer chemical lifetime, like CO, than the characteristic time of turbulent mixing in the PBL [around 15 min in a well-mixed boundary layer; see Stull (1988)]. A simplified model (model 1) of a constant CO VMR in the PBL can be assumed using the ground-level in situ measurements and the PBL height provided, respectively, by the CO11M and the CAML. The lower parts of the a priori CO profile (see Fig. 7) are modified from the ground to the top of the PBL. Strong constraints are imposed in the retrieval algorithm to keep a constant mixing ratio in these lower layers. The CO total column is retrieved with these new assumptions. Both retrievals are in good agreement: the newly and previously retrieved total columns differ by only 3% and the residuals of the two fits are similar. Without any pollution contamination assumption from other emission sites, model 1 provides the highest value that can be reached by the CO partial column in the PBL.

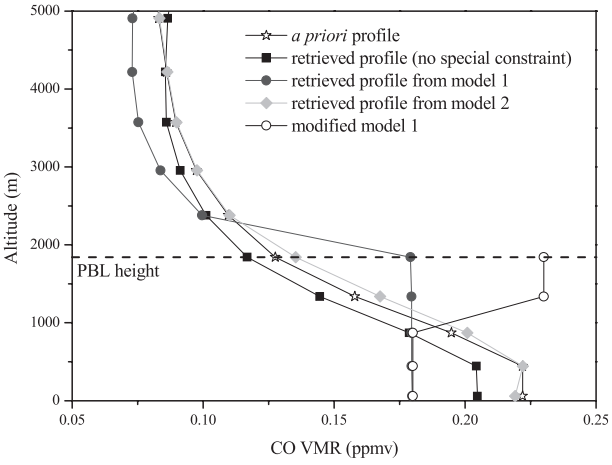

FIG. 7. Low parts of the different profiles used by the models described in section 4c for a PBL top of 1800 m.

3) MODEL 2 DESCRIPTION

Local emissions of pollutants from the ground during the day need time to reach the free troposphere and the higher atmospheric layers. The VMR vertical profile in the free troposphere (and above) can be assumed to be reasonably unchanged during the whole day (assuming no significant variation through long-range transport of air masses). To detect local emissions in the PBL, other constraints are added to force the VMR profile above the PBL top (model 2) fixed at the concentration given by the a priori profile. With this assumption, any diurnal change in CO should be attributable to local ground emissions in the PBL only observed by ground-level in situ measurements (see section 4b).

4) MODELS DISCUSSION

Table 3 shows the CO partial columns in the PBL obtained for three time periods by the different models—no specific constraints, model 1, and model 2 (cf. Fig. 7):

- The first case with a PBL top of 350 m corresponds to the daily pollution peak period (around 0730 UTC, with an in situ measurement of 0.43 ppmv).
- The second case is the average one (around 1015 UTC) with a PBL top of 1200 m and a CO in situ VMR of 0.24 ppmv.
- The last one is a background case (around 1230 UTC) with a 1800-m PBL height and 0.18 ppmv of CO.

The agreement between no specific constraints and model 1 is reasonably satisfying (within the errors bars) and demonstrates the acceptable sensitivity of the QualAir FTS in the PBL. For example, at 1030 UTC the partial column obtained with model 1 is $(6.1 \pm 1.1) \times 10^{17}$ molecules per square centimeter compared to 5.4×10^{17}

TABLE 3. CO partial column in the PBL obtained with different assumptions (10^{17} molecules per square centimeter). In parenthesis, the retrieved ground VMR with these assumptions (for model 1, they are the mean values measured by the CO11M analyzer, in boldface).

	Partial column in PBL (ground retrieved VMR in ppmv)		
	Height at 350 m	Height at 1200 m	Height at 1800 m
No specific constraints	2.08 (0.25)	5.36 (0.22)	6.76 (0.21)
Model 2	2.28 (0.29)	5.69 (0.24)	7.70 (0.23)
Model 1	2.98 ± 0.40 (**0.43**)	6.14 ± 1.10 (**0.24**)	7.08 ± 1.90 (**0.18**)
Modified model 1			7.84 ± 1.90 (**0.20**)

molecules per square centimeter (retrieved with the CO standard a priori profile). Model 2 improves the agreement of the CO partial column in the PBL with the local estimations (model 1) in the case of higher pollution levels (see the green open stars in Fig. 5, bottom panel).

For the background case (Table 3 last column), the model 2 partial column in the PBL is higher than that of model 1. The discrepancy can be explained by the underestimation of model 1 due to the pollution contamination from the west of the Ile de France at 1200 UTC (cf. Fig. 8). Figure 8 shows the forecasts of the CO VMR at 600-m height for 1 July 2009 (left panel for 0600 UTC and right panel for 1200 UTC). These maps were obtained by Prévisions et Observations de la Qualité de l'Air en France et en Europe (PREV'AIR) using CHIMERE (http://www.prevair.org/fr/index.php) and provided during the 2009 Megacities: Emissions, Urban, Regional and Global Atmospheric Pollution and Climate Effects, and Integrated Tools for Assessment and Mitigation (MEGAPOLI) campaign (http://megapoli.lisa.univ-paris12.fr). No strong pollution of CO can be observed around the Ile de France for the first recorded spectrum at 0641 UTC (the east pollution is too far to be measured by the QualAir FTS). For 1230 UTC, the solar azimuth angle is about 200°, providing an observation direction of south-southwest. The QualAir FTS line of sight crossed the pollution from the west at high altitudes in the PBL. We have taken into account this pollution contamination effect in model 1 by adding 50 ppbv in the two last levels of the PBL (230 ppbv at 1.336 and 1.843 km and 180 ppbv below; see the open circles in Fig. 7). The 50 ppbv is the difference between 0600 and 1200 UTC in the PREV'AIR maps. With these assumptions, the partial column in the PBL is 7.81×10^{17} molecules per square centimeter, which agrees with the results from model 2. This partial column in the PBL can be obtained using model 1 (without any modification) with 200 ppbv of CO for each level (against 180 ppbv). This shows the importance and the difficulty in choosing the ground VMR value correctly for model 1 because of the strong spatial variability of the CO ground VMR in urban areas; whereas model 2 needs to combine different independent observations, but it improves the CO urban emission monitoring in the PBL.

We show here the good consistency of model 2, which improves the QualAir FTS sensitivity in the PBL. Next,

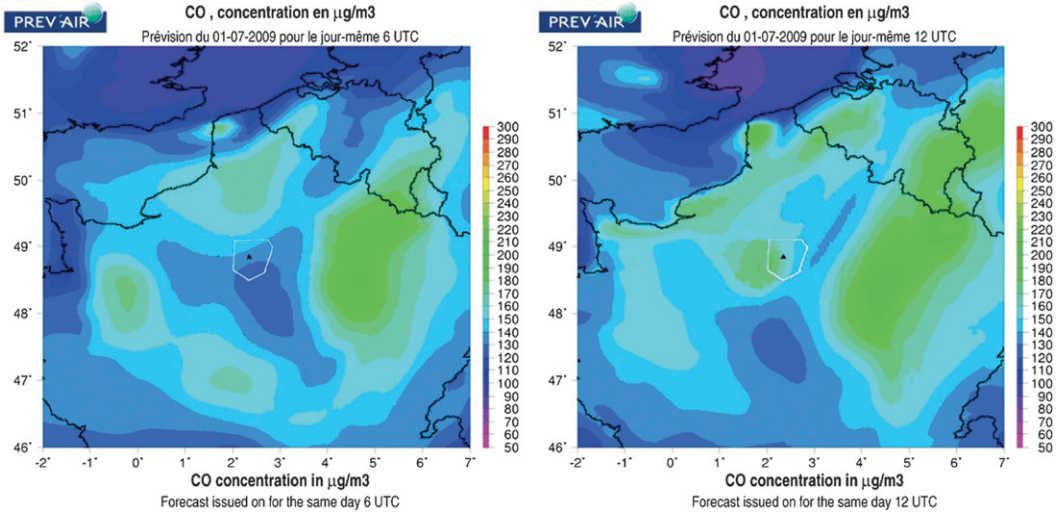

FIG. 8. Forecasts of CO VMR at 600-m height for 1 Jul 2009 by PREV'AIR using CHIMERE during 2009 MEGAPOLI (without aircraft trajectories).

in order to detect local variability or emission of the atmospheric pollution in the PBL more precisely, we have to generate a set of a priori profiles that are as correct as possible to the reality obtained monthly from the QualAir FTS results and atmospheric models such as WACCM. More studies (different species, more sophisticated models, etc.) are planned to improve the capabilities and the synergy of the QualAir instruments to retrieve the PBL partial columns.

5. Conclusions

This paper has presented an instrumental description of the QualAir FTS and has provided results on N_2O, CH_4, and CO. A good correlation between N_2O and CH_4 is observed as expected in the case of the Paris megacity where there are no specific sources for these two species. No correlation of these long-lived tracers with CO is noticed because of the highly variable urban anthropogenic emission of CO from the traffic and industry. Comparison with MetOp IASI total columns shows a good consistency when similar atmospheric air masses are compared. More detailed and specific comparisons will be made during future studies for different atmospheric conditions (pollution levels, seasons, etc.), as well as comparisons with atmospheric models. There is good coincidence of the CO ground VMR measured by the QualAir FTS and the in situ CO11M analyzer—good agreement in time for the daily pollution peak, the same decreasing trend during the day, and a similar CO background value except for the absolute value of the pollution peak, which probably results from the different techniques employed by these two instruments and the difference between an in situ (local) and a remote sensing (more integrated along the line of sight) measurement. Even if information contained in the solar spectra is merging atmospheric layers, the QualAir FTS sensitivity is good enough to retrieve the PBL partial column correctly. Under the assumption of no contamination from the free troposphere (and above) by local emissions, the characterization of the daytime local emission of CO is improved. Future investigations for updated VMR data will be led to describe the local variability of CO over the Paris area more precisely.

Overall, this paper has demonstrated the good performances of the QualAir FTS and the high capabilities of the various instruments of the QualAir platform. The complementarity of these instruments offers a promising synergy that lead to more systematic air quality studies.

Acknowledgments. Funding support was provided by the Université Pierre et Marie Curie. We are also grateful for the support and facilities of Institut Pierre-Simon Laplace. IASI has been developed and built under the responsibility of the CNES. It is flown onboard the MetOp satellite as part of the Eumetsat Polar System (EPS). The IASI L1 data are received through the Eumetcast near-real-time data distribution service. IASI L1 and L2 data are stored in the Ether French atmospheric database (http://ether.ipsl.jussieu.fr).

REFERENCES

Barret, B., M. De Mazière, and E. Mahieu, 2003: Ground-based FTIR measurements of CO from the Jungfraujoch: Characterisation and comparison with in situ surface and MOPITT data. *Atmos. Chem. Phys.,* **3,** 2217–2223.

Blumstein D., and Coauthors, 2004: IASI instrument: Technical overview and measured performances. *Infrared Spaceborne Remote Sensing XII,* M. Strojnik, Ed., International Society for Optical Engineering (SPIE Proceedings, Vol. 5433), doi:10.1117/12.560907.

Clerbaux, C., and Coauthors, 2009: Monitoring of atmospheric composition using the thermal infrared IASI/MetOp sounder. *Atmos. Chem. Phys.,* **9,** 6041–6054.

Clough, S. A., M. W. Shephard, E. J. Mlawer, J. S. Delamere, M. J. Lacono, K. Cady-Pereira, S. Boukabara, and P. D. Brown, 2005: Atmospheric radiation transfer modelling: A summary of the AER codes, short communication. *J. Quant. Spectrosc. Radiat. Transfer,* **91,** 233–244.

Delmas, R., G. Mégie, and V.-H. Puech, 2005: *Physique et Chimie de l'Atmosphère*. Belin, 640 pp.

Duchatelet, P., and Coauthors, 2010: Hydrogen fluoride total and partial column time series above the Jungfraujoch from long-term FTIR measurements: Impact of the line-shape model, error budget, seasonal cycle and comparison with satellite and model data. *J. Geophys. Res.,* **115,** D22306, doi:10.1029/2010JD014677.

Fischer, H., F. G. Wienhold, P. Hoor, O. Bujok, C. Schiller, P. Siegmund, and J. Lelieveld, 2000: Trace correlations in northern high latitude lowermost stratosphere: Influence of cross-tropopause mass exchange. *Geophys. Res. Lett.,* **27,** 97–100.

George, M., and Coauthors, 2009: Carbon monoxide distributions from the IASI/METOP mission: Evaluation with other space-borne sensors. *Atmos. Chem. Phys.,* **9,** 8317–8330.

Hase, F., T. Blumenstock, and C. Paton-Walsh, 1999: Analysis of the instrumental line shape of high-resolution Fourier transform IR spectrometers with gas cell measurements and new retrieval software. *Appl. Opt.,* **38,** 3417–3422.

——, J. W. Hannigan, M. T. Coey, A. Goldman, M. Höpfner, N. B. Jones, C. P. Rinsland, and S. W. Wood, 2004: Intercomparison of retrieval codes used for the analysis of high-resolution: Ground-based FTIR measurements. *J. Quant. Spectrosc. Radiat. Transfer,* **87,** 25–52.

——, P. Demoulin, A. J. Sauval, G. C. Toon, P. F. Bernath, A. Goldman, J. W. Hannigan, and C. P. Rinsland, 2006: An empirical line-by-line model for the infrared solar transmittance spectrum from 700 to 5000 cm^{-1}. *J. Quant. Spectrosc. Radiat. Transfer,* **102,** 450–463, doi:10.1016/j.jqsrt.2006.02.026.

Honoré, C., and Coauthors, 2008: Predictability of European air quality: Assessment of 3 years of operational forecasts and analyses by the PREV'AIR system. *J. Geophys. Res.,* **113,** D04301, doi:10.1029/2007JD008761.

Kondo, Y., U. Schmidt, T. Sugita, A. Engel, M. Koike, P. Aimedieu, M. R. Gunson, and J. Rodriguez, 1996: NO_y correlation with N_2O and CH_4 in the midlatitude stratosphere. *Geophys. Res. Lett.,* **23,** 2369–2372.

Meier, A., G. C. Toon, C. P. Rinsland, A. Goldman, and F. Hase, 2004: Spectroscopic atlas of atmospheric microwindows in the middle Infra-red. 2nd ed. IRF Tech. Rep. 048, 612 pp. [Available online at http://documents.irf.se/get_document.php?group=Administration&docid=1217.]

Menut, L., C. Flamant, J. Pelon, and P. H. Flamant, 1999: Urban boundary-layer height determination from lidar measurements over the Paris area. *Appl. Opt.,* **38,** 945–954.

Michelsen, H. A., G. L. Manney, M. R. Gunson, C. P. Rinsland, and R. Zander, 1998: Correlations of stratospheric abundances of CH_4 and N_2O derived from ATMOS measurements. *Geophys. Res. Lett.,* **25,** 2777–2780.

Park, J. H., 1983: Analysis method for Fourier transform spectroscopy. *Appl. Opt.,* **22,** 835–849.

Plumb, R. A., and M. K. W. Ko, 1992: Interrelationships between mixing ratios of long-lived stratospheric constituents. *J. Geophys. Res.,* **97** (D9), 10 145–10 156.

Rinsland, C. P., and Coauthors, 1998: Northern and Southern Hemisphere ground-based infrared spectroscopic measurements of tropospheric carbon monoxide and ethane. *J. Geophys. Res.,* **103,** 28 197–28 217.

——, and Coauthors, 1999: Infrared solar spectroscopic measurements of free tropospheric CO, C_2H_6, and HCN above Mauna Loa, Hawaii: Seasonal variations and evidence for enhanced emissions from the Southeast Asian tropical fires of 1997-1998. *J. Geophys. Res.,* **104,** 18 667–18 680.

——, E. Mahieu, R. Zander, P. Demoulin, J. Forrer, and B. Buchmann, 2000: Free tropospheric CO, C_2H_6, and HCN above central Europe: Recent measurements from the Jungfraujoch station including the detection of elevated columns during 1998. *J. Geophys. Res.,* **105,** 24 235–24 249.

——, A. Goldman, J. W. Elkins, L. S. Chiou, J. W. Hannigan, S. W. Wood, E. Mahieu, and R. Zander, 2006: Long-term trend of CH_4 at northern mid-latitudes comparison between ground-based infrared solar and surface sampling measurements. *J. Quant. Spectrosc. Radiat. Transfer,* **97,** 457–466.

——, ——, J. W. Hanniganc, S. W. Wood, L. S. Chiou, and E. Mahieu, 2007: Long-term trends of tropospheric carbon monoxide and hydrogen cyanide from analysis of high resolution infrared solar spectra. *J. Quant. Spectrosc. Radiat. Transfer,* **104,** 40–51.

Rodgers, C. D., 1990: Characterization and error analysis of profile retrieved from remote sensing measurements. *J. Geophys. Res.,* **95,** 5587–5595.

Rothman, L. S., and Coauthors, 2009: The HITRAN 2008 molecular spectroscopic database. *J. Quant. Spectrosc. Radiat. Transfer,* **110,** 533–572.

Schmidt, H., C. Derognat, R. Vautard, and M. Beekmann, 2001: A comparison of simulated and observed ozone mixing ratios for the summer of 1998 in western Europe. *Atmos. Environ.,* **35,** 6277–6297.

Schneider, M., and F. Hase, 2008: Technical note: Recipe for monitoring of total ozone with a precision of around 1 DU applying mid-infrared solar absorption spectra. *Atmos. Chem. Phys.,* **8,** 63–71.

——, and ——, 2009: Improving spectroscopic line parameters by means of atmospheric spectra: Theory and example for water vapor and solar absorption spectra. *J. Quant. Spectrosc. Radiat. Transfer,* **110,** 1825–1839, doi:10.1016/j.jqsrt.2009.04.011.

——, ——, and T. Blumenstock, 2006: Water vapour profiles by ground-based FTIR spectroscopy: Study for an optimised retrieval and its validation. *Atmos. Chem. Phys.,* **6,** 811–830.

——, K. Yoshimura, F. Hase, and T. Blumenstock, 2010: The ground-based FTIR network's potential for investigating the atmospheric water cycle. *Atmos. Chem. Phys.,* **10,** 3427–3442.

Stull, R. B., 1988: *An Introduction to Boundary Layer Meteorology*. Springer, 441–497 pp.

Sussmann, R., W. Stremme, J. P. Burrows, A. Richter, W. Seiler, and M. Rettinger, 2005: Stratospheric and tropospheric NO_2 variability on the diurnal and annual scale: A combined retrieval from ENVISAT/SCIAMACHY and solar FTIR at the Permanent Ground-Truthing Facility Zugspitze/Garmisch. *Atmos. Chem. Phys.,* **5,** 2657–2677.

Té, Y., P. Jeseck, S. Payan, I. Pépin, and C. Camy-Peyret, 2008: The Fourier transform spectrometer of the QualAir platform. *Eighth Atmospheric Spectroscopy Applications Proc.,* Reims, France, 6–9.

——, ——, ——, ——, and ——, 2010: The Fourier transform spectrometer of the UPMC University QualAir platform. *Rev. Sci. Instrum.,* **81,** 103102, doi:10.1063/1.3488357.

Tournier, B., D. Blumstein, F.-R. Cayla, and G. Chalon, 2002: IASI level 0 and 1 processing algorithms description. *Proc. 12th Int. TOVS Study Conf. (ITSC-XII)*, Lorne, VIC, Australia, TOVS Working Group.

Turquety, S., and Coauthors, 2007: Inventory of boreal fire emissions for North America in 2004: The importance of peat burning and pyro-convective injection. *J. Geophys. Res.,* **112,** D12S03, doi:10.1029/2006JD007281.

U.S. Air Force, 1976: U.S. Standard Atmospheric Tables 1976. U.S. Government Printing Office.

Vautard, R., M. Beekmann, J. Roux, and D. Gombert, 2001: Validation of a hybrid forecasting system for the ozone concentrations over the Paris area. *Atmos. Environ.,* **35,** 2449–2461.

Wunch, D., C. Midwinter, J. R. Drummond, C. T. McElroy, and A.-F. Bagès, 2006: University of Toronto's balloon-borne Fourier transform spectrometer. *Rev. Sci. Instrum.,* **77,** 093104, doi:10.1063/1.2338289.

Zhao, Y., and Coauthors, 1997: Carbon monoxide column abundances and tropospheric concentrations retrieved from high resolution ground-based infrared solar spectra at 43.5°N over Japan. *J. Geophys. Res.,* **102** (D19), 23 403–23 411.

——, and Coauthors, 2002: Spectroscopic measurements of tropospheric CO, C_2H_6, C_2H_2, and HCN in northern Japan. *J. Geophys. Res.,* **107,** 4343, doi:10.1029/2001JD000748.